

Enhancement of Segregated Finite Element Method with Adaptive Meshing Technique for Viscous Incompressible Thermal Flow Analysis

Nippon Wansophark*, Pramote Dechaumphai*

Department of Mechanical Engineering, Faculty of Engineering, Chulalongkorn University, Patumwan, Bangkok, Thailand, 10330.

*Corresponding author, E-mails: nippon.w@eng.chula.ac.th, fmepdc@eng.chula.ac.th

Received 2 Aug 2002

Accepted 12 Dec 2002

ABSTRACT A segregated finite element algorithm is combined with a monotone streamline upwinding method for solving two-dimensional viscous incompressible thermal flow problems. The finite element equations are derived from a set of coupled nonlinear Navier-Stokes equations that consist of the conservation of mass, momentums and energy. The method uses the three-node triangular element with equal-order interpolations for all the variables of the velocity components, the pressure and the temperature. The finite element formulation is validated by developing a corresponding computer program and evaluated by examples of viscous incompressible thermal flows. These examples are the thermally driven flows in a square cavity and in the concentric cylinders. In addition, an adaptive meshing technique is also combined with the finite element algorithm to further increase solution accuracy, and at the same time, to minimize the computational time and computer memory requirement.

KEYWORDS: finite element method, streamline upwinding, adaptive meshing technique, segregated algorithm.

INTRODUCTION

The main difficulties for viscous incompressible thermal flow analysis can be classified into two categories: (a) the complex coupling between the energy equation and the equations governing the fluid motion, and (b) the non-linear phenomenon of the convection terms in both the momentum equations and the energy equation. One successful technique for solving couple partial differential equations, such as the governing equations of fluid flow, is known as the SIMPLER (Semi-Implicit Method for Pressure-Linked Equations Revised) algorithm¹, which compute the primitive variables, namely the velocity components, the pressure and the temperature, separately. The algorithm, originally devised for finite difference method, has been modified and proposed by several researchers for the finite element method.²⁻⁴ In computing the convection terms, the widely used technique is known as streamline upwinding method. One successful method was reported by Rice and Schnipke⁵ using the four-node quadrilateral element. The method evaluates convection terms directly along the local streamlines. Calculations presented in their papers have shown that the method is monotonic and introduces artificial numerical diffusion. The effect of numerical diffusion is to smear the solution in area of high flow field gradients and hence decreases the solution accuracy.

The accuracy in a numerical solution is an important factor that must be considered especially for large scale problems. The solution accuracy can be increased by using small elements in the computational domain, but it will require additional computer time and data storage.⁶ To reduce such difficulty, a technique of adaptive meshing⁷⁻⁸ is incorporated in the computational algorithm.

In this paper, the procedure for computing the convection terms in the momentum equations and the energy equation along local streamlines passing through triangular elements is presented. Triangular elements are employed in order to combine effectively with the adaptive meshing technique presented herein. These triangular elements use equal-order interpolation functions for the velocity components, the pressure and the temperature to reduce the complexity in deriving the corresponding finite element equations. A segregated solution algorithm⁹⁻¹⁰ is also incorporated to compute the velocity components, pressure and temperature separately for further improving the computational efficiency. In addition, the adaptive meshing technique is applied to reduce the computational time as well as the computer memory. The technique places small elements in the regions of large change in the solution gradients to increase solution accuracy, and at the same time, places larger elements in the other regions to reduce the

computational time. The paper describes briefly the set of the partial differential equations that satisfy the law of conservation of mass, momentums and energy. Corresponding finite element equations are derived and element matrices presented. The computational procedure used in the development of the computer program and the basic idea behind the adaptive meshing technique are then described. Finally, the finite element formulation and the computer program are verified using examples that have prior numerical solutions and experimental results.

THEORETICAL FORMULATION AND SOLUTION PROCEDURE

Governing Equations

The fundamental laws used to solve two-dimensional, steady state, viscous incompressible thermal flow behavior consist of: (a) the law of conservation of mass which is called the continuity equation, (b) the law of conservation of momentums, and (c) the law of conservation of energy, as follows,

$$\frac{\partial u}{\partial x} + \frac{\partial v}{\partial y} = 0 \quad (1a)$$

$$\rho \left[u \frac{\partial u}{\partial x} + v \frac{\partial u}{\partial y} \right] = -\frac{\partial p}{\partial x} + \mu \left[\frac{\partial^2 u}{\partial x^2} + \frac{\partial^2 u}{\partial y^2} \right] \quad (1b)$$

$$\rho \left[u \frac{\partial v}{\partial x} + v \frac{\partial v}{\partial y} \right] = -\frac{\partial p}{\partial y} + \mu \left[\frac{\partial^2 v}{\partial x^2} + \frac{\partial^2 v}{\partial y^2} \right] - \rho g (1 - \beta(T - T_o)) \quad (1c)$$

$$\rho c \left[u \frac{\partial T}{\partial x} + v \frac{\partial T}{\partial y} \right] = k \left[\frac{\partial^2 T}{\partial x^2} + \frac{\partial^2 T}{\partial y^2} \right] \quad (1d)$$

where u and v are the velocity components in the x and y direction, respectively, ρ is the density, p is the pressure, μ is the viscosity, g is the gravitational acceleration constant, β is the volumetric coefficient of thermal expansion, T is the temperature, T_o is the reference temperature for which buoyant force in the y -direction vanishes, c is the specific heat, and k is the coefficient of thermal conductivity.

Finite Element Formulation

The three-node triangular element is used in this study. The element assumes linear interpolation for the velocity components, the pressure, and the temperature as,

$$u(x, y) = N_i u_i \quad (2a)$$

$$v(x, y) = N_i v_i \quad (2b)$$

$$p(x, y) = N_i p_i \quad (2c)$$

$$T(x, y) = N_i T_i \quad (2d)$$

where

$i = 1, 2, 3$, and N_i is the element interpolation functions.

The basic idea of the solution algorithm presented in this paper is to use the two momentum equations for solving both of the velocity components, use the continuity equation for solving the pressure, and use the energy equation for solving the temperature. The finite element equations corresponding to the momentum, the continuity and the energy equations are shown in next section.

Discretization of Momentum Equations

The two momentum equations, Eqs. (1b-c), are discretized using the conventional Bubnov-Galerkin method. However, a special treatment for the convection terms is incorporated. These terms are approximated by a monotone streamline upwinding formulation for using with the triangular element.¹¹ In this approach, the convection terms in the form,

$$u \frac{\partial \phi}{\partial x} + v \frac{\partial \phi}{\partial y} \quad (3)$$

which are related to the transport variable, ϕ , are first rewritten in the streamline coordinates as,

$$U_s \frac{\partial \phi}{\partial s} \quad (4)$$

where U_s and $\partial/\partial s$ are the velocity and the gradient along the streamline direction, respectively. For pure convection, the term in Eq. (4) is constant along the streamline. These terms are evaluated by a streamline tracing method which keeps track the direction of the flow within the element.

Using the standard Galerkin approach, each momentum equation is multiplied by weighting functions, N_i , and then the diffusion terms are integrated by parts using the Gauss theorem¹² to yield the element equations in the form,

$$[A]\{u\} = \{R_{px}\} + \{R_u\} \quad (5a)$$

$$[A]\{v\} = \{R_{py}\} + \{R_v\} + \{R_b\} \quad (5b)$$

where the coefficient matrix $[A]$ contains the known contributions from the convection and diffusion terms.

The load vectors on the right-hand side of Eqs (5a-b) are defined by,

$$\{R_{px}\} = - \int_{\Omega} \{N_i\} \frac{\partial p}{\partial x} d\Omega \quad (6a)$$

$$\{R_{py}\} = - \int_{\Omega} \{N_i\} \frac{\partial p}{\partial y} d\Omega \quad (6b)$$

$$\{R_u\} = \mu \int_{\Gamma} \{N_i\} \left[\frac{\partial u}{\partial x} n_x + \frac{\partial u}{\partial y} n_y \right] d\Gamma \quad (6c)$$

$$\{R_v\} = \mu \int_{\Gamma} \{N_i\} \left[\frac{\partial v}{\partial x} n_x + \frac{\partial v}{\partial y} n_y \right] d\Gamma \quad (6d)$$

$$\{R_b\} = - \int_{\Omega} \{N_i\} [\rho g (1 - \beta(T - T_o))] d\Omega \quad (6e)$$

where Ω is the element area and Γ is the element boundary. The element equations are assembled to yield the global equations for the velocity components. Such global equations are then modified for the specified velocity components along the boundaries prior to solving for the new velocity components.

Discretization of Pressure Equation

To derive the discretized pressure equation, the method of weighted residuals is applied to the continuity equation, Eq (1c),

$$\int_{\Omega} N_i \left(\frac{\partial u}{\partial x} + \frac{\partial v}{\partial y} \right) d\Omega = - \int_{\Omega} \left(\frac{\partial N_i}{\partial x} u + \frac{\partial N_i}{\partial y} v \right) d\Omega + \int_{\Gamma} N_i (u n_x + v n_y) d\Gamma = 0 \quad (7)$$

where the integrations are performed over the element domain Ω and along the element boundary Γ and n_x and n_y are the direction cosines of the unit vector normal to element boundary with respect to x and y direction, respectively. As mentioned earlier, the continuity equation is used for solving the pressure, but the pressure term does not appear in the continuity equation. For this reason, the relation between velocity components and pressure are thus required. Such relations can be derived from the momentum equations, Eqs (5a-b) as,

$$A_{ii} u_i = - \sum_{j \neq i} A_{ij} u_j + f_i^u - \int_{\Omega} N_i \frac{\partial p}{\partial x} d\Omega \quad (8a)$$

$$A_{ii} v_i = - \sum_{j \neq i} A_{ij} v_j + f_i^v - \int_{\Omega} N_i \frac{\partial p}{\partial y} d\Omega \quad (8b)$$

where f_i^u and f_i^v are the surface integral terms and the source term due to buoyancy. By assuming constant pressure gradient on an element, then,

$$u_i = \hat{u}_i - K_i^p \frac{\partial p}{\partial x} \quad (9a)$$

$$v_i = \hat{v}_i - K_i^p \frac{\partial p}{\partial y} \quad (9b)$$

where

$$\hat{u}_i = \frac{- \sum_{j \neq i} A_{ij} u_j + f_i^u}{A_{ii}} \quad (10a)$$

$$\hat{v}_i = \frac{- \sum_{j \neq i} A_{ij} v_j + f_i^v}{A_{ii}} \quad (10b)$$

$$K_i^p = \frac{\int_{\Omega} N_i d\Omega}{A_{ii}} \quad (10c)$$

by applying the element velocity interpolation functions, Eqs. (2a-b), into the continuity equation, Eq (7),

$$- \int_{\Omega} \frac{\partial N_i}{\partial x} (N_j u_j) d\Omega - \int_{\Omega} \frac{\partial N_i}{\partial y} (N_j v_j) d\Omega + \int_{\Gamma} N_i (u n_x + v n_y) d\Gamma = 0 \quad (11)$$

and introducing the nodal velocities u_j and v_j from Eqs. (9a-b), then Eq (11) becomes,

$$\int_{\Omega} \frac{\partial N_i}{\partial x} (N_j K_j^p) \frac{\partial p}{\partial x} d\Omega + \int_{\Omega} \frac{\partial N_i}{\partial y} (N_j K_j^p) \frac{\partial p}{\partial y} d\Omega = \int_{\Omega} \frac{\partial N_i}{\partial x} (N_j \hat{u}_j) d\Omega + \int_{\Omega} \frac{\partial N_i}{\partial y} (N_j \hat{v}_j) d\Omega - \int_{\Gamma} N_i (u n_x + v n_y) d\Gamma \quad (12)$$

Finally, applying the element pressure interpolation functions, Eq (2c), the above element equations can be written in matrix form with unknowns of the nodal pressures as,

$$[K_x + K_y]\{p\} = \{F_u\} + \{F_v\} + \{F_b\} \quad (13)$$

where

$$[K_x] = \int_{\Omega} \left\{ \frac{\partial N_i}{\partial x} \right\} (N_j K_j^p) \left[\frac{\partial N_i}{\partial x} \right] d\Omega \quad (14a)$$

$$[K_y] = \int_{\Omega} \left\{ \frac{\partial N_i}{\partial y} \right\} (N_j K_j^p) \left[\frac{\partial N_i}{\partial y} \right] d\Omega \quad (14b)$$

$$\{F_u\} = \int_{\Omega} (N_j \hat{u}_j) \left[\frac{\partial N_i}{\partial x} \right] d\Omega \quad (14c)$$

$$\{F_v\} = \int_{\Omega} (N_j \hat{v}_j) \left[\frac{\partial N_i}{\partial y} \right] d\Omega \quad (14d)$$

$$\{F_b\} = - \int_{\Gamma} \{N_i\} (u n_x + v n_y) d\Gamma \quad (14e)$$

The above element pressure equations are assembled to form the global equations. Boundary conditions for the specified nodal pressures are imposed prior to solving for the updated nodal pressures.

Discretization of Energy Equation

The energy equation is derived using an approach which is similar to the momentum equations. The streamline upwinding method is applied to the convection term in the energy equation. The standard Galerkin method is then applied to yield the element equations which can be written in matrix form as,

$$[K] \{T\} = \{R\} \quad (15)$$

where the matrix [K] consists of the contributions from the convection and diffusion terms, and the load matrix {R} represents the heat flux along the element boundary as,

$$\{R\} = k \int_{\Gamma} \{N_i\} \left[\frac{\partial T}{\partial x} n_x + \frac{\partial T}{\partial y} n_y \right] d\Gamma \quad (16)$$

These element equations are again assembled to yield the global temperature equations. Appropriate boundary conditions are applied prior to solving for the new temperature values.

Computational Procedure

The computational procedure is illustrated in Fig 1. A set of initial nodal velocity components, pressures, and temperatures are first assumed. The new nodal

temperatures are computed using Eq (15). The new nodal velocity components and pressures are then computed using Eqs (5a-b) and Eq (13), respectively. The nodal velocity components are then updated using Eqs (8a-b) with the computed nodal pressures. This process is continued until the specified convergence criterion is met. Such segregated solution procedure helps reducing the computer storage because the equations for the velocity components, the pressure, and the temperature are solved separately.

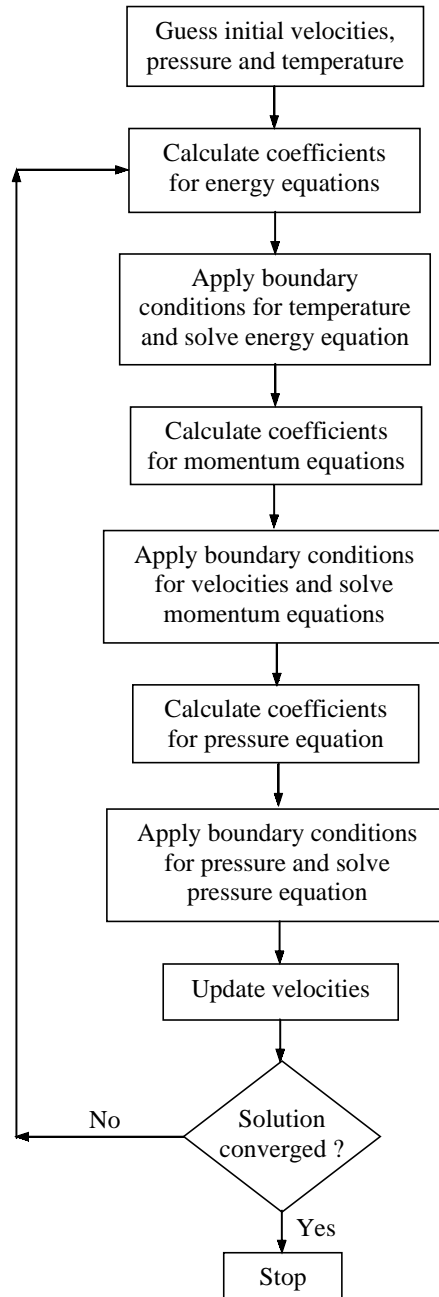


Fig 1. Schematic diagram of the computational procedure.

ADAPTIVE MESHING TECHNIQUE

The idea behind the adaptive meshing technique presented herein is to construct a new mesh based on the solution obtained from the previous mesh. The new mesh consists of small elements in the regions with large change in solution gradients and larger elements in the other regions where the change in solution gradients is small. To determine proper element sizes at different locations in the flow field, the solid-mechanics concept for determining the principal stresses from a given state of stresses at a point is employed. Since small elements are needed in the regions where the high value of heat flux occurs, thus the flow temperature can be used as an indicator for the determination of proper element sizes.

To determine proper element sizes, the second derivatives of the temperature with respect to the global coordinates x and y are first computed,

$$\begin{bmatrix} \frac{\partial^2 T}{\partial x^2} & \frac{\partial^2 T}{\partial x \partial y} \\ \frac{\partial^2 T}{\partial x \partial y} & \frac{\partial^2 T}{\partial y^2} \end{bmatrix} \quad (17)$$

The principal quantities in the principal directions X and Y where the cross derivatives vanish, are then determined,

$$\begin{bmatrix} \frac{\partial^2 T}{\partial X^2} & 0 \\ 0 & \frac{\partial^2 T}{\partial Y^2} \end{bmatrix} \quad (18)$$

The magnitude of the larger principal quantity is then selected,

$$\lambda = \max \left(\left| \frac{\partial^2 T}{\partial X^2} \right|, \left| \frac{\partial^2 T}{\partial Y^2} \right| \right) \quad (19)$$

This value is used to compute proper element size, h , at that locations from the condition¹³,

$$h^2 \lambda = \text{constant} = h_{\min}^2 \lambda_{\max} \quad (20)$$

where h_{\min} is the specified minimum element size, and λ_{\max} is the maximum principal quantity for the entire model.

Based on the condition shown in Eq. (20), proper element sizes are generated according to the given minimum element size h_{\min} . Specifying too small h_{\min} may result in a model with an excessive number of elements. On the other hand, specifying too large h_{\min}

may result in an inadequate solution accuracy or excessive analysis and remeshing cycles. These factors must be considered prior to generating a new mesh.

RESULTS

In this section, two example problems are presented. The first example, thermally driven cavity flow, is chosen to evaluate the finite element formulation and to validate corresponding computer program with previously published results. The second example, thermally driven flow in concentric cylinders, is presented to illustrate the capability of the adaptive meshing technique for the analysis of viscous incompressible thermal flow.

Thermally Driven Cavity Flow

The first example for evaluating the finite element formulation and validating the developed computer program is the problem of free convection in a square enclosure. The square enclosure (Fig 2) is bounded by the two vertical walls with specified temperatures of 20°C and 60°C and insulated along the top and bottom surfaces. The problem was analyzed by the penalty finite element method¹⁴ for which the result can be used for comparison. The finite element model consisting of 2,809 nodes and 5,408 elements, is used in this study. Fig 3 and 4 show the predicted velocity vectors and temperature contours, respectively, for the case with the Rayleigh number of 10^4 . The figures show relatively smooth velocity vectors of the flow that circulates in the counterclockwise direction and the smooth temperature distribution. The same analysis is repeated but with the Rayleigh number of 10^5 . Different flow patterns of the velocity vectors and temperature

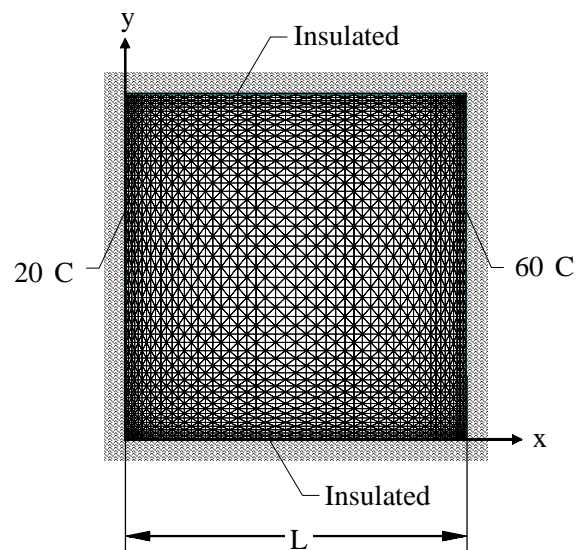


Fig 2. Finite element model and boundary conditions of thermally driven cavity flow.

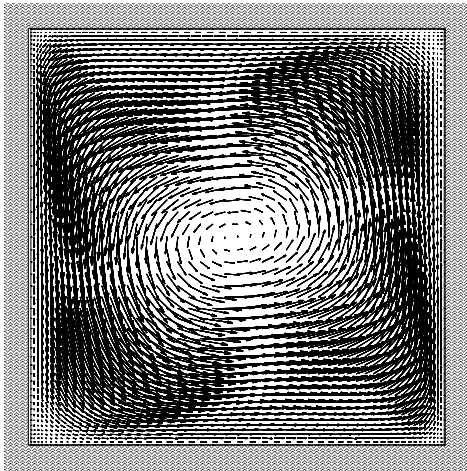


Fig 3. Predicted velocity vectors of thermally driven cavity flow at $Ra = 10^4$.

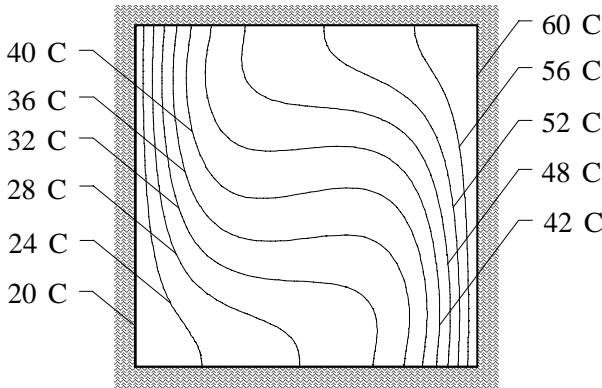


Fig 4. Predicted temperature contours of thermally driven cavity flow at $Ra = 10^4$.

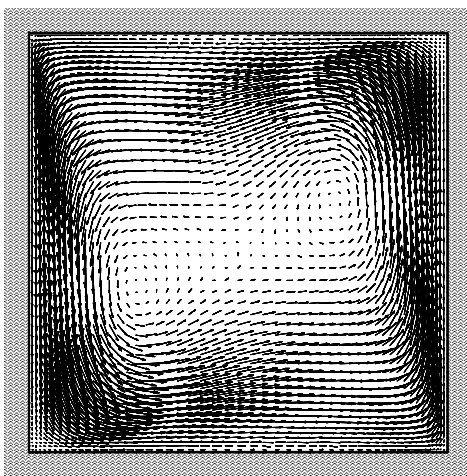


Fig 5. Predicted velocity vectors of thermally driven cavity flow at $Ra = 10^5$.

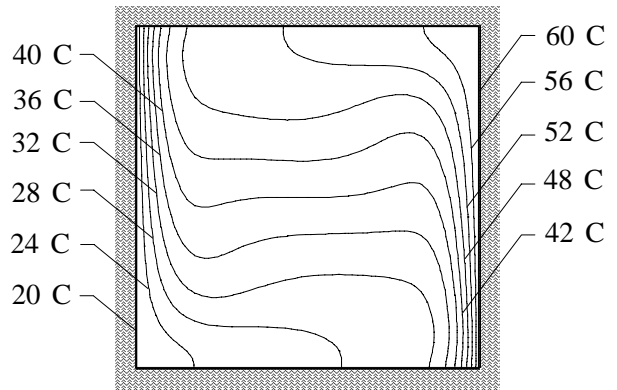


Fig 6. Predicted temperature contours of thermally driven cavity flow at $Ra = 10^5$.

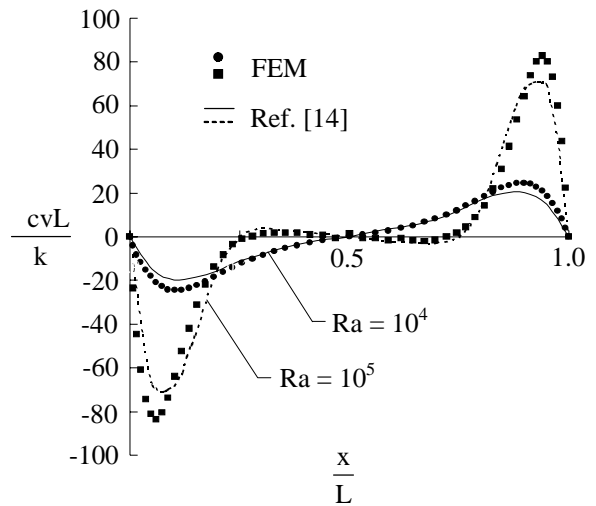


Fig 7. Comparative velocity profiles along the mid-height of the square enclosure.

contours are obtained as shown in Fig 5 and 6. The flow velocity pattern indicates two regions of circulation, both in counterclockwise direction. The predicted velocity profiles and the temperature distributions along the mid-height of the square enclosure for both flow cases are compared with the results from Ref. [14] as shown in Fig 7 and 8, respectively. The figures show good agreement of the solutions for both the flow cases.

Thermally Driven Flow in Concentric Cylinders

To demonstrate the capability of the combination of adaptive meshing technique with the finite element method, the problem of thermally driven flow in concentric cylinders is selected. The fluid is freely convected in the annular space between long, horizontal concentric cylinders due to high temperature on the inner cylinder and lower temperature on the outer

cylinder (Fig 9). This problem was previously studied by experiment¹⁵ for which the result can be used for comparison. The comparison of the results presented herein are at Rayleigh number of 4.7×10^4 and Prandtl number of 0.706 with a ratio of gap width to inner-cylinder diameter (L/D) of 0.8.

Due to symmetry of the flow solution, only the right half of the concentric cylinders is analyzed. The adaptive meshing technique starts from creating a relatively uniform mesh as shown in Fig 10. This initial mesh consists of 1,045 nodes and 1,942 elements. The figure also shows the predicted temperature contours on the left half.

The numerical solution obtained from the initial mesh is then used to construct the second adaptive mesh as described in Section 3. The second adaptive mesh and the predicted temperature contours are shown in Fig 11. The figure shows smaller elements are generated in the region near the cylinder surfaces where large change in temperature gradients occurs.

The entire procedure is repeated again to generate the third adaptive mesh and the predicted temperature

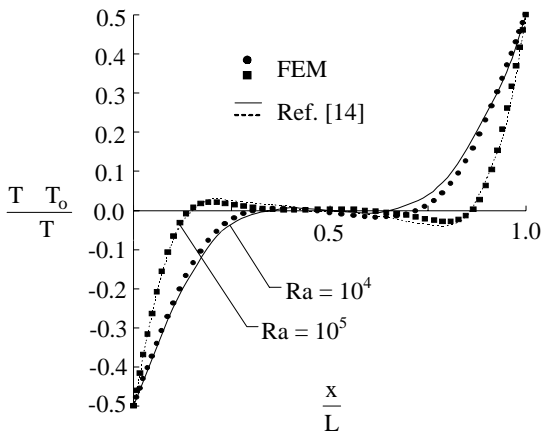


Fig 8. Comparative temperature distribution along the mid-height of the square enclosure.

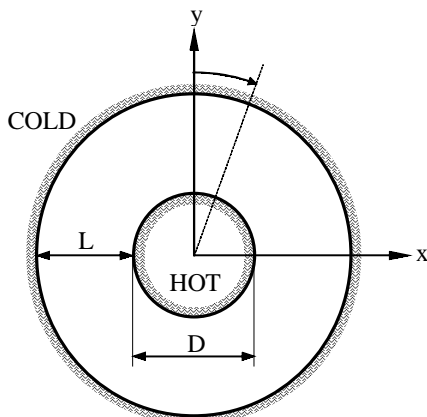


Fig 9. Thermally driven flow in concentric cylinders.

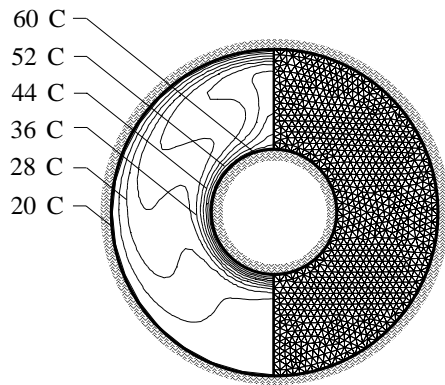


Fig 10. First finite element mesh and the predicted temperature contours.

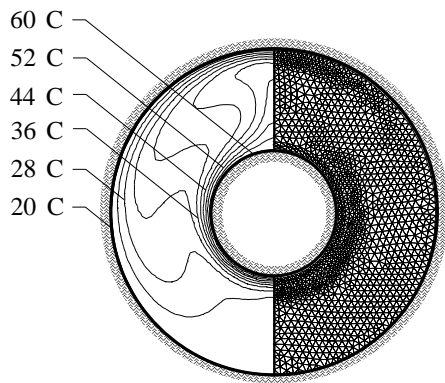


Fig 11. Second finite element mesh and the predicted temperature contours.

contours as shown in Fig 12. Fig 13 shows the comparisons of the equivalent conductivities between the initial and the third adaptive meshes at the inner and outer cylinder surfaces with the experimental results. The equivalent conductivity is defined as the actual heat flux divided by the heat flux that would occur by pure conduction in the absence of fluid motion. The figure shows the adaptive mesh provides higher solution accuracy compared to the experimental results because small elements are generated automatically in the regions of complex flow behavior.

CONCLUSIONS

This paper presents the development of the streamline upwinding finite element method using the three-node triangular element for the analysis of viscous incompressible thermal flow problems. The presented solution algorithm employs equal-order interpolation functions for the velocity components, pressure and temperature of the triangle. The finite element formulation and its computational procedure are first described. The procedure uses a segregated solution algorithm to compute the velocities, pressure and

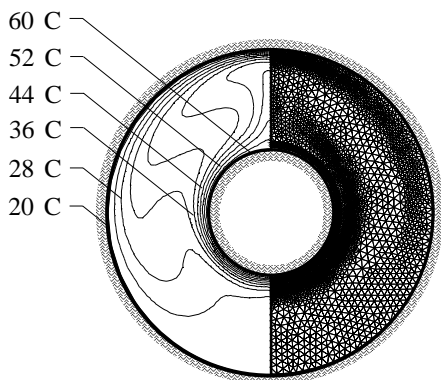


Fig 12. Third finite element mesh and the predicted temperature contours.

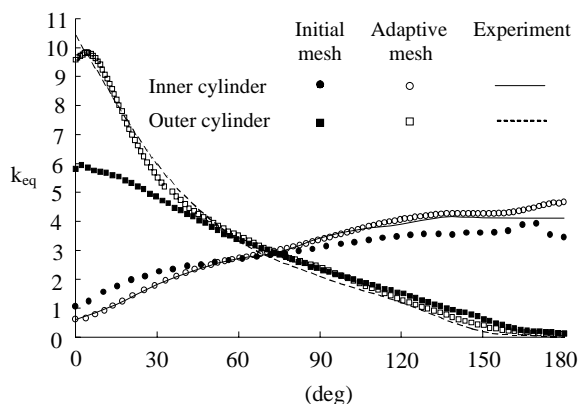


Fig 13. Comparison of the experimental and numerical local equivalent conductivities.

temperature separately for improving the computational efficiency. A streamline upwinding formulation is applied to the convection terms in the momentum and the energy equations to suppress the non-physical spatial oscillation in the numerical solutions. The corresponding finite element equations are derived and a corresponding computer program has been developed. The finite element method is combined with an adaptive meshing technique to improve the flow solution accuracy. The adaptive meshing technique generates an entirely new mesh based on the solution obtained from a previous mesh. The new mesh consists of clustered elements in the regions with large change in the temperature gradients to provide higher solution accuracy. And at the same time, larger elements are generated in the other regions to reduce the computational time and the computer memory. The capability of the finite element solution algorithm and the corresponding computer program has been evaluated by examples that have prior numerical solutions and experimental results. The combined finite element solution algorithm and the adaptive meshing technique has demonstrated the

efficiency of the entire process for improved solution accuracy at the reduced computer memory and computational time.

ACKNOWLEDGEMENTS

The authors are pleased to acknowledge the Thailand Research Fund (TRF) for supporting this research work.

REFERENCES

1. Patankar SV (1980) Numerical Heat Transfer and Fluid Flow, Hemisphere, Washington DC.
2. Prakash C and Patankar SV (1985) A Control Volume-Based Finite-Element Method for Solving the Navier-Stokes Equations Using Equal-Order Velocity-Pressure Interpolation. *Numerical Heat Transfer* **8**, 259-80.
3. Ramaswamy B and Jue TC (1991) A Segregated Finite Element Formulation of Navier-Stokes Equations Under Laminar Conditions. *Finite Elements in Analysis and Design* **9**, 257-70.
4. Haroutunian V, Engelman MS and Hasbani I (1993) Segregated Finite Element Algorithms for the Numerical Solution of Large-Scale Incompressible Flow Problems. *International Journal for Numerical Methods in Fluids* **17**, 323-48.
5. Rice JG and Schnipke RJ (1985) A Monotone Streamline Upwind Finite Element Method for Convection-Dominated Flows. *Computer Methods in Applied Mechanics and Engineering* **48**, 313-27.
6. Zienkiewicz OC, Liu YC, and Huang GC (1989) Error Estimates and Convergence Rates for Various Incompressible Elements. *International Journal for Numerical Methods in Engineering* **28**, 2191-202.
7. Peraire J, Vahjdati M, Morgan K, and Zienkiewicz OC (1987) Adaptive Remeshing for Compressible Flow Computation. *Journal of Computational Physics* **72**, 449-66.
8. Dechaumphai P (1995) Adaptive Finite Element Technique for Heat Transfer Problems. *Journal of Energy, Heat and Mass Transfer* **17**, 87-94.
9. Rice JG and Schnipke RJ (1986) An Equal-Order Velocity-Pressure Formulation that does not Exhibit Spurious Pressure Modes. *Computer Methods in Applied Mechanics and Engineering* **58**, 135-49.
10. Choi HG and Yoo JY (1994) Streamline Upwind Scheme for the Segregated Formulation of the Navier-Stokes Equation. *Numerical Heat Transfer, Part B* **25**, 145-61.
11. Wansophark N (2000) Adaptive Meshing Technique for Viscous Flow Analysis Using Equal-Order Triangular Element, Master Thesis, Mechanical Engineering, Faculty of Engineering, Chulalongkorn University.
12. Dechaumphai P (1999) Finite Element Method in Engineering, 2nd ed, Chulalongkorn University Press, Bangkok.
13. Oden JT and Carey GF (1981) Finite Elements: Mathematical Aspects, Prentice-Hall, Englewood Cliffs, New Jersey.
14. Reddy JN and Satake A (1980) A Comparison of a Penalty Finite Element Model with the Stream Function-Vorticity Model of Natural Convection in Enclosures. *Journal of Heat Transfer* **102**, 659-66.
15. Kuehn TH and Goldstein RJ (1976) An Experimental and Theoretical Study of Natural Convection in the Annulus Between Horizontal Concentric Cylinders. *Journal of Fluid Mechanics* **74**, 695-719.